The Interaction Between Invariant Natural Killer T Cells and B Cells in Adipose Tissue

A Senior Thesis Presented to
The Faculty of the Department of Molecular Biology,
Colorado College

By
Abigail Kumagai
Bachelor of Arts Degree in Molecular Biology
May/2016

Dr. Olivia Hatton
Primary Thesis Advisor

Dr. Darrell Killian
Secondary Thesis Advisor

Abstract

Invariant natural killer T cells (iNKT) cells can play an anti-inflammatory role and secrete the cytokine interleukin 10 (IL-10). IL-10 acts to inhibit signaling from inflammatory cytokines. Loss of iNKT cells has been implicated in cancer, autoimmune diseases, diabetes, and obesity. During early responses to immune challenge, iNKT cells provide help to B cells via two main pathways. Direct help from iNKT cells to B cells follows an innate pathway, while indirect help from iNKT cells to B cells follows an adaptive pathway. The specific interaction between B cells and iNKT cells within adipose tissue is not understood. Here, the interaction between iNKT cells and B cells within white adipose tissue and brown adipose tissue was examined using αGalCer, a potent stimulator of iNKT cells. In both brown and white adipose tissue, αGalCer stimulation resulted in an expansion of tissue-resident, IL-10 producing iNKT cells. However, tissue-resident B cells did not significantly increase in number or IL-10 production. Instead, a population of $B220^{+}CD19^{-}CD1d^{+}$ lymphocytes were found to have an iNKT-dependent expansion in response to αGalCer. Our data suggests that iNKT cells provide indirect, adaptive help to B cells within both brown and white adipose tissue. These findings have implications in possible treatments for diabetes and obesity, as activated iNKT cells could be used to reduce tissue inflammation.

Introduction

Invariant Natural Killer T Cells (iNKT cells)

Invariant natural killer T cells (iNKT cells) are lymphocytes that regulate a wide variety of immune cells, and consequently play a critical role in a number of pathologies. iNKT cells have been implicated in autoimmune diseases such as diabetes, lupus and multiple sclerosis**.** For example, activated iNKT cells were found to reduce paralysis in experimental autoimmune encephalomyelitis, a murine model of multiple sclerosis (Singh et al., 2001). An increase in iNKT cell numbers was also associated with a lower risk of developing diabetes in non-obese diabetic mice (Tard et al., 2015). iNKT cells have also been implicated in cancer, weight loss and have potential as vaccine targets (Leadbetter et al., 2011, Lynch et al., 2012). Nanoparticles designed to specifically target and activate iNKT cells are currently being tested for new cancer therapies, as iNKT cells induce anti-tumor mechanisms (Macho-Fernandez et al., 2014).

iNKT cells are a subset of T cells which display characteristics similar to Natural Killer cells (NK cells; Lynch et al., 2014). They are named invariant for their T cell receptor (TCR) which has an α-chain (V_α14-J_α18) paired with V_β8.2 or V_β7 or V_β2 TCRβ chains (Leadbetter et al., 2011). iNKT cells can be found in the spleen, peripheral blood, liver and adipose tissue. In visceral adipose tissue iNKT cells compose 15-20% of the total T cell population (Lynch et al., 2012). iNKT cells which produce the anti-inflammatory cytokine interleukin-10 (IL-10) have been found to be a distinct regulatory subset of iNKT cells (Lynch et al., 2015).

iNKT cells are activated by an interaction between their invariant TCR and CD1d, an antigen presenting complex found on B cells and most professional antigen presenting cells, including dendritic cells. CD1d is composed of a large hydrophobic channel which binds and presents glyocolipids to iNKT cells. One of the glyocolipids bound by CD1d is the ligand α-galactosylceramide (αGalCer). Originally isolated from sea sponges, synthetic α-GalCer is currently used to activate iNKT cells *in vitro* and *in vivo* (Leadbetter et al., 2011).

B Cells

B cell lymphocytes are integral to the immune system's defense against pathogens, and subsequent memory and immunity. When mature naive B cells receive activating signals through the B cell receptor (BCR), a subset differentiates to become antibody producing plasmablasts, while the majority of activated B cells enter a structure of lymphoid tissues known as the germinal center (Nutt et al., 2015). Within the germinal center, B cells receive additional signals, notably through CD40 on $CD4^+$ T cells. The combination of signals from the BCR and CD40 drives B cell proliferation, somatic hypermutation, affinity maturation, and antibody class-switching. B cells then exit the germinal center as differentiated antibody-producing plasma cells or long-lived memory B cells, both with the ability to produce high affinity antibodies of the appropriate isotype (Recaldin & Fear, 2015).

A subset of B cells has been found to produce the anti-inflammatory cytokine interleukin-10 (IL-10). These B cells have been termed regulatory B cells (B_{regs}) or B10 cells. Within the spleen, only 1-2% of B cells are capable of

producing IL-10 following stimulation (Nishimura et al., 2013). The signals required for development of B10 cells is actively under investigation, and multiple subsets of B10 cells are thought to exist. This IL-10 producing population of B cells plays an anti-inflammatory role and loss of these cells has been implicated in inflammatory bowel disease, diabetes, lupus, and multiple sclerosis (Tedder, 2015).

Innate and Adaptive Interactions Between B Cells and iNKT Cells

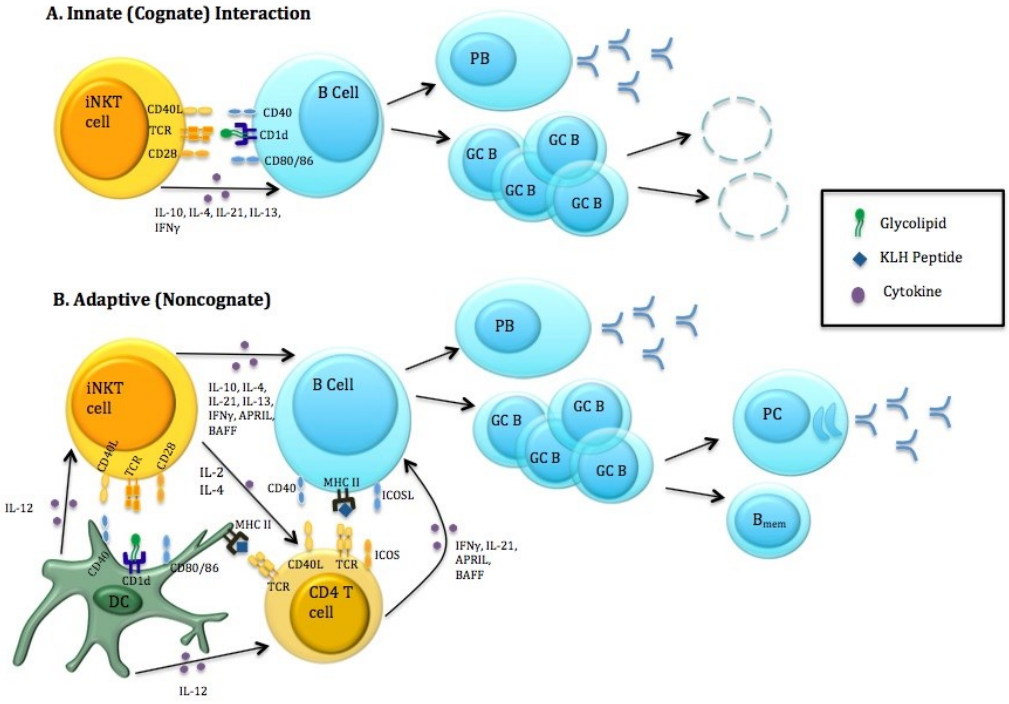

Figure 1 | Invariant Natural Killer T Cells are involved in innate (cognate) and adaptive (noncognate) pathways which serve to activate B cells. These pathways have primarily been studied in the spleen, where B cells differentiate into plasmablasts (PB) and germinal center B cells (GC B) following activation. Innate help (**A**) begins when a B cell presents a glycolipid loaded in CD1d to an iNKT cell. The iNKT cell then supplies signals such as IFNγ, IL-21, CD40L and CD28 in order to activate the B cell. However this activation only results in plasmablast and germinal center B cell development, and lacks development of plasma cells (PC) or memory B cells (B_{mem}). Additionally an innate response is specific to T-dependent type II antigens. Adaptive help (**B**) results in the creation of both plasma cells and memory B cells. iNKT cells recruit dendritic cells (DC) and CD4 T cells first in order to activate protein specific B cells. The dendritic cell presents a glycolipid loaded into CD1d to an iNKT cell. The iNKT cell then supplies signals, such as CD40L and CD28, which cause the dendritic cell to upregulate MHC class II antigen presentation and CD40 molecules in order to activate CD4 T cells. CD4 T cells can also receive direct signals from iNKT cells, such as IL-2, IL-4, BAFF and APRIL. The CD4 T cells then activate B cells to differentiate and ultimately form memory B cells. (Modified from Leadbetter et al., 2014)

Studies of the iNKT and B cell interaction in the spleen have led to two models for B cell activation by iNKT cells (Figure 1; Leadbetter et. al., 2014). These innate and adaptive models of iNKT help provided to B cells result in different outcomes in terms of antibody production and memory generation. iNKT cells can directly interact with B cells in the innate model of iNKT cell help (Figure

1A). In this model, the iNKT cell recognizes the glycolipid and CD1d molecules presented on the B cell. The iNKT cell then activates the B cell directly by signals from CD40L and CD28 and the secretion of cytokines such as IL-21 and IFNγ. The notable difference between innate and adaptive iNKT help is that innate iNKT help results exclusively in the production of plasmablasts and does not result in the production of a humoral memory response and plasma cells (Figure 1A) (Chang et al., 2012).

In adaptive iNKT help (Figure 1B) the iNKT cell initially interacts with glycolipid bound CD1d presented by a dendritic cell. iNKT binding sends signals to the dendritic cell through CD40L and CD28, resulting in increased major histocompatibility complex class II (MHC II) presentation by the dendritic cell. The dendritic cell can then interact with and activate $CD4^+$ T cells, which in turn activates antigen-specific B cells. Thus, adaptive iNKT help results in the production of a humoral memory response and the production of class-switched antibodies. The exact reason for this difference in outcome is not entirely understood, but is thought to allow iNKT cells to participate in an early response to a pathogen via an innate pathway, and to be involved in later responses which subsequently create humoral memory (Leadbetter et al., 2014). While these models for iNKT help in B cell activation have been developed in the spleen, B cells and iNKT cells also reside within adipose tissue. However, the exact mechanisms behind their interaction within adipose tissue is not fully understood.

Adipose-Resident Lymphocytes

Traditionally, adipose tissue has been divided into two forms – white adipose tissue (WAT) and brown adipose tissue (BAT). White adipose tissue serves as triglyceride energy storage and brown adipose tissue serves an important role in thermoregulation (Park et al., 2014). While white adipose tissue tends to be the primary focus of obesity studies, brown adipose tissue has been found to play an important role in weight loss and blood sugar regulation (Wu et al., 2014). Both white and brown adipose tissue have been found to have tissue resident lymphocyte populations, some of which are phenotypically different from lymphocytes in other tissue types (Exley et al., 2014). White adipose tissue resident iNKT cells have been identified. These iNKT cells produce interleukin 10 (IL-10) and interleukin 2 (IL-2) and serve to regulate inflammation (Lynch et al., 2014). Adipose tissue resident B cells have also been identified, and they too produce IL-10 and serve an anti-inflammatory purpose (Nishimura et al., 2013).

iNKT Cells in Obesity

A major pathology of obesity is a chronic state of inflammation within adipose tissue (Apostolopoulos et al., 2015). This state of inflammation is perpetuated by anti-inflammatory immune cells, which convert to a pro-inflammatory phenotype, and release pro-inflammatory cytokines such as tumor necrosis factor α (TNFα; Wentworth et al., 2010). Adipocytes then fail to correctly store the excess lipids within inflamed tissue, and resistance to insulin subsequently develops, leading to metabolic dysfunction. iNKT cell numbers drop

as obesity progresses, and are restored with loss of weight (Lynch et al., 2012). When iNKT cells are transferred into obese mice, the mice not only lose weight but also improve insulin sensitivity (Lynch et al., 2012). Finally, iNKT cell activation by αGalCer injection in obese mice also results in loss of weight and improved insulin sensitivity (Lynch et al., 2012). These findings suggest that iNKT cells play an important role in maintaining homeostasis within adipose tissue, and that their regulatory nature can help to reduce tissue inflammation, even after inflammation has begun.

Interactions Between iNKT Cells and B Cells in Adipose Tissue

B cells and iNKT cells are both found within adipose tissue, and appear to have distinct regulatory phenotypes. The mechanisms and kinetics behind their interaction in adipose tissue is not fully understood. Additionally, most studies on iNKT and B cell populations in adipose tissue have focused on white adipose tissue, as it makes up the majority of adipose tissue in mammals. The presence of functional brown adipose tissue in adult humans has only recently been appreciated (Betz & Enerback, 2015). Understanding how these iNKT cells and B cells interact and the means by which they are activated within both white and brown adipose tissue is critical to furthering therapies and treatments for obesity and glucose intolerance. In this study, we aimed to address how adipose iNKT cells and B cells interact, if these interactions are similar to those in the spleen or are unique to adipose tissue, and whether B cell activation was iNKT-dependent in adipose tissue.

Results

iNKT cells and B cells co-localize in WAT and spleen

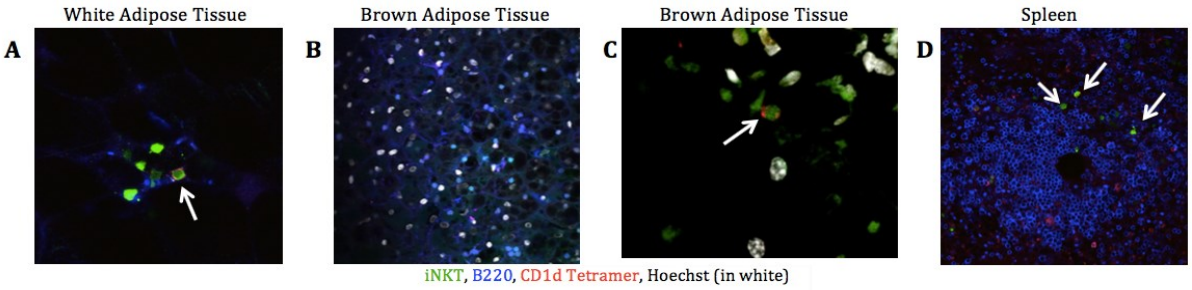

Figure 2 | Confocal microscope images of adipose and splenic tissue. iNKT reporter mice (C57BL/6 Cxcr6 GFP$^{+/-}$) tissue samples were used, and CD1d Tetramer staining was used as a secondary confirmation for iNKT cells. White arrows point to iNKT cells. B cells are tagged with B220 and appear blue. A Hoechst stain was used to stain DNA in the brown adipose tissue. (**A**) shows iNKT cells and B cells in white adipose tissue, (**B**) shows B cells in brown adipose tissue, (**C**) shows an iNKT cell in brown adipose tissue, outlined in red CD1d Tetramer, and (**D**) shows B cells and iNKT cells in the spleen

iNKT cells and B cells are readily found in the spleen (Leadbetter et al., 2011) and white adipose (Lynch et al., 2014). However the presence of iNKT cells in brown adipose tissue has been less thoroughly examined. iNKT cells from C57BL/6 *Cxcr6* $^{GFP/-}$ mice, which express eGFP in any cell bearing high levels of CXCR6, the majority of which are iNKT cells, were visualized in combination with B cells in white adipose tissue (Figure 2A), brown adipose tissue (Figure 2B, C), and the spleen (Figure 2D) using confocal microscopy. iNKT cells were also identified by their ability to bind CD1d tetramer on their surface (Figure 2A, white arrow). However the CD1d tetramer at times exhibited nonspecific binding (Figure 2B, D) making it difficult to work with. iNKT cells are present in white adipose tissue, brown adipose tissue, and in the spleen (Figures 2A, C, D white arrows). B220^{+} B cells are also present in the white adipose tissue, brown adipose tissue and spleen (Figures 2A, B, D blue cells). In the

white adipose tissue samples, iNKT cells and B cells were co-localized (Figure 2A). In the brown adipose tissue both B cells and iNKT cells were observed in the same tissue sample, (Figure 2B, C) however no images were taken of the two cell types in close proximity. Finally in the spleen an abundance of B cells was visualized, along with a few iNKT cells in very close proximity (Figure 2D). The co-localization of iNKT cells and B cells in the white adipose tissue and spleen indicates the potential for a direct interaction between those cells within those tissue types.

Adipose Lymphocytes are optimally isolated by Collagenase IV digestion

One of the difficulties in studying iNKT and B cell interactions in the adipose tissue is isolating the relatively low number of adipose resident lymphocytes. A number of methods utilizing different Collagenases have been described in the literature, including Collagenase VIII (Valina et al., 2007), Collagenase I (Huang et al., 2013) and Collagenase IV (Lynch et al., 2014). Cell count estimations using Trypan blue staining, and percentages of iNKT cells and B cells assessed by flow cytometry data were used to determine efficiency of the Collagenase-mediated isolation of lymphocytes (data not shown). Collagenase IV proved to be more effective on both brown and white adipose tissue, whereas Collagenase VIII worked well on BAT, but not on WAT (data not shown). Collagenase IV solution with FCS serum displayed higher lymphocyte cell yields (data not shown) than Collagenase IV alone in both adipose tissues. Therefore,

the Collagenase IV solution with 5% FCS serum was used throughout the experiments to isolate adipose-resident lymphocytes.

Adipose iNKT cells proliferate markedly following αGalCer injection

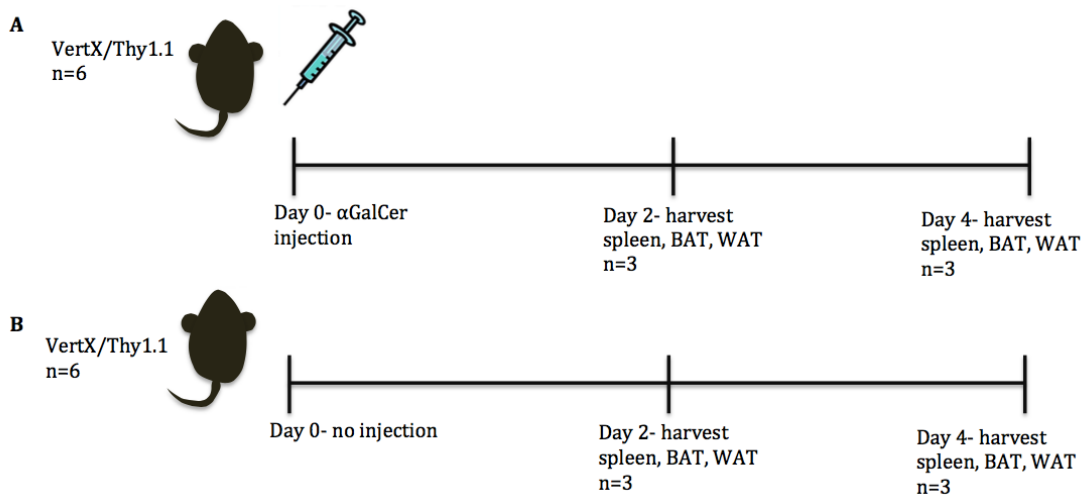

Figure 3 | Mice injection strategy with αGalCer for tissue harvesting at day 2 and day 4. Six VertX/Thy1.1 mice were injected with αGalCer on day 0 (**A**), and six uninjected VertX/Thy1.1 mice were used as controls (**B**). VertX/Thy1.1 strains are reporter mice for the cytokine interleukin 10 (IL-10). Mice were harvested at two time points following injection, day 2 and day 4 for comparison of IL-10 production.

VertX/Thy1.1 mice were used to examine the kinetics of B cell and iNKT cell activation following injection with αGalCer (Figure 3). These mice express GFP when the gene encoding the anti-inflammatory cytokine interleukin-10 (IL-10) is transcribed (Madan et al., 2009). Mice received intravenous injections of 0.5 μg αGalCer on day 0. Tissues were harvested on day 2 and day 4 (Figure 4). Noninjected VertX/Thy1.1 mice were used as controls.

Flow Cytometry Gating Strategy for Detection of iNKT Cells, B Cells and IL-10

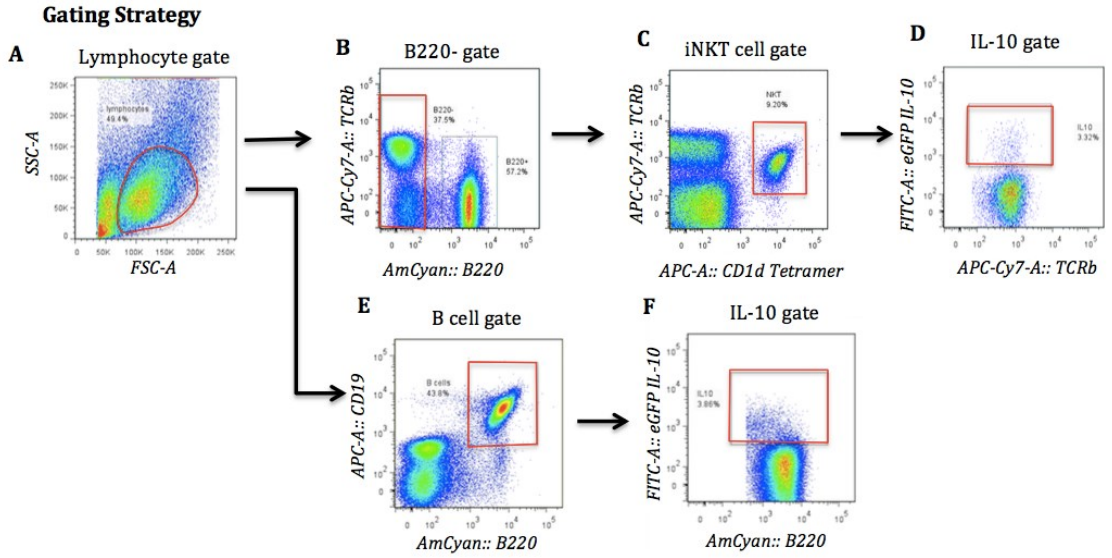

Figure 4 | Gating strategy for invariant natural killer T cells and B cells. Prior to the lymphocyte gate (**A**), doublets were gated out using a linear gate on forward scatter area versus forward scatter height. Dead cells were then excluded using a propidium iodide (PI) stain. iNKT cells were gated as $B220^-$ (**B**) and $TCRb^+CD1d\text{-}Tetramer^+$ (**C**). $IL\text{-}10^+$ iNKT cells are shown in (**D**). B cells were gated as $B220^+CD19^+$ (**E**), and $IL\text{-}10^+$ B cells are shown in (**F**).

Tissue-resident lymphocytes were examined by flow cytometry (Figure 4). iNKT cells were defined as $B220^-TCR\beta^+CD1d\text{-}Tetramer^+$ cells (Figure 4B, C). B cells were defined as cells positive for both $B220^+CD19^+$ (Figure 4A, E).

Adipose and splenic iNKT cell population expand following αGalCer injection

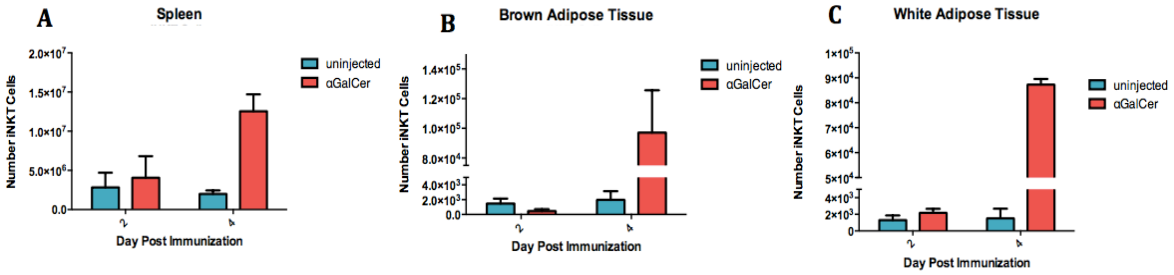

Figure 5 | iNKT cell population numbers increase in the spleen, brown adipose tissue and white adipose tissue 4 days after αGalCer injection. Red bars indicate mice that received αGalCer injection (n=3), blue indicates uninjected mice (n=3). The cells counts were calculated from flow cytometry percentage data of iNKT cells in VertX/Thy1.1 mice on day 2 and day 4 following αGalCer injection. The number of iNKT cells in the spleen (**A**), brown adipose tissue (**B**), and white adipose tissue (**C**) expand following αGalCer injection.

In all tissue types iNKT cell numbers were unchanged two days post injection (Figure 5). iNKT cells expand greatly in all tissue types by day four post αGalCer injection (Figure 5). On day four, the mean number of iNKT cells in the spleen increased six-fold (Figure 5A), however iNKT cells in the adipose tissue displayed the most marked increase. The mean number of brown adipose tissue iNKT cells expanded 49 fold (Figure 5B) and the mean number of white adipose tissue iNKT cells expanded 57 fold (Figure 5C).

Adipose B cell populations do not expand following αGalCer injection

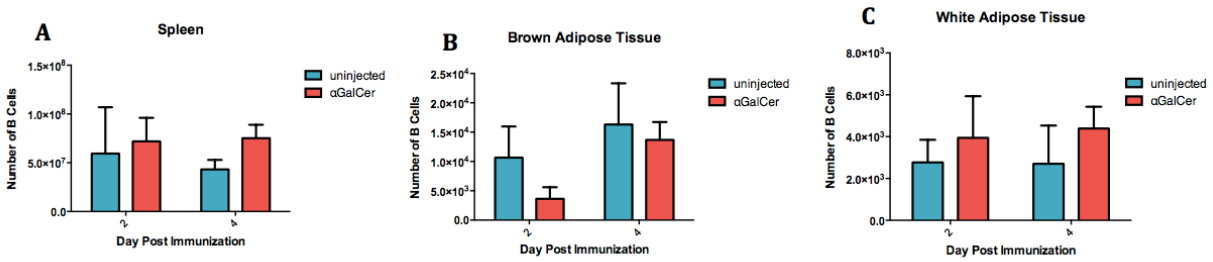

Figure 6 | B cell population numbers in the spleen, brown adipose tissue and white adipose tissue do not notably increase following αGalCer injection. Red bars indicate mice that received αGalCer injection (n=3), blue indicates uninjected mice (n=3). The cells counts were calculated from flow cytometry percentage data of B cells in VertX/Thy1.1 mice on day 2 and day 4 following αGalCer injection. Number of $B220^{+}CD19^{+}$ B cells are shown for the spleen (**A**), brown adipose tissue (**B**), and white adipose tissue (**C**).

No remarkable increase in B cell population was observed in any of the tissue types 2 days after αGalCer injection (Figure 6). Four days after αGalCer injection, the mean B cell population in the spleen increased 1.7 fold (Figure 6A). There is no notable change in B cell numbers in the adipose tissue four days after αGalCer injection (Figure 6B, C), especially given the standard error.

IL-10 producing iNKT cells increase 4 days after αGalCer injection

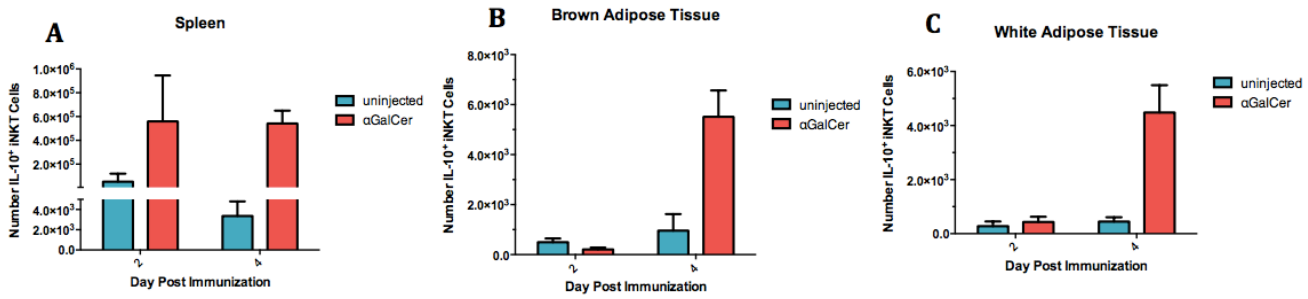

Figure 7 | IL-10 producing iNKT cell numbers increase in the spleen, brown adipose tissue, and white adipose tissue 4 days post αGalCer injection. Red bars indicate mice that received αGalCer injection (n=3), blue indicates uninjected mice (n=3). The cell counts were calculated from flow cytometry percentage data of IL-10$^+$ invariant natural killer T cells in VertX/Thy1.1 mice on day 2 and day 4 following αGalCer injection. IL-10 producing iNKT cell numbers are shown in the spleen (**A**), brown adipose tissue (**B**), and white adipose tissue (**C**).

Regulatory iNKT cells and regulatory B cells serve an anti-inflammatory function via secretion of the cytokine interleukin-10 (IL-10) (Lynch et al., 2015) (Nishimura et al., 2013). iNKT cells producing IL-10 were identified as B220$^-$ TCRβ$^+$CD1d-Tetramer$^+$eGFP$^+$ (Figure 4A-D). None of the tissue types had a significant change in IL-10 production from iNKT cells at day two post αGalCer injection. However, in all three tissues (spleen, brown adipose and white adipose) a notable increase in iNKT cells producing IL-10 was found at day four post αGalCer injection. The mean population of splenic IL-10 producing iNKT cells increased 161 fold following αGalCer stimulation (Figure 7A). The mean brown adipose tissue IL-10 producing iNKT cell population expanded five fold (Figure 7B) and the mean population of white adipose tissue IL-10 producing iNKT cells increased 10 fold (Figure 7C).

IL-10+ B cells display no change in adipose tissue in response to αGalCer injection

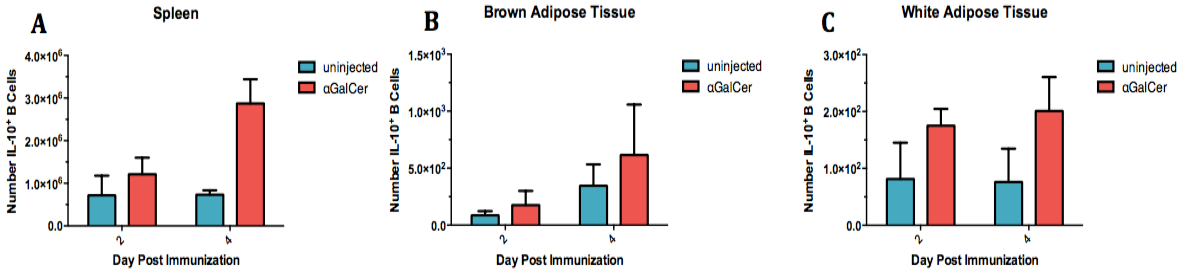

Figure 8 | IL-10 producing B cell numbers increase in the spleen (**A**) 4 days post αGalCer injection. Brown adipose tissue (**B**), and white adipose tissue (**C**) IL-10$^+$ B cells display a less significant increase following αGalCer stimulation. Red bars indicate mice that received αGalCer injection (n=3), blue indicates uninjected mice (n=3). The cell counts were calculated from flow cytometry percentage data of IL-10$^+$ B cells in VertX/Thy1.1 mice on day 2 and day 4 following αGalCer injection.

Populations of B cells producing IL-10 were identified as B220$^+$CD19$^+$eGFP$^+$ (Figure 4A, E, F). The spleen, brown adipose tissue and white adipose tissue all had minimal increases in IL-10 producing B cells two days post αGalCer injection. By day 4 post αGalCer injection, the mean number of splenic B cells producing IL-10 increased almost four fold (Figure 8A). However, in the brown adipose tissue (Figure 8B) and white adipose tissue (Figure 8C) the number of IL-10$^+$ B cells increased by a small amount, if at all, by day four post injection.

CD1d^{+} Regulatory B cells increase on day four post αGalCer stimulation

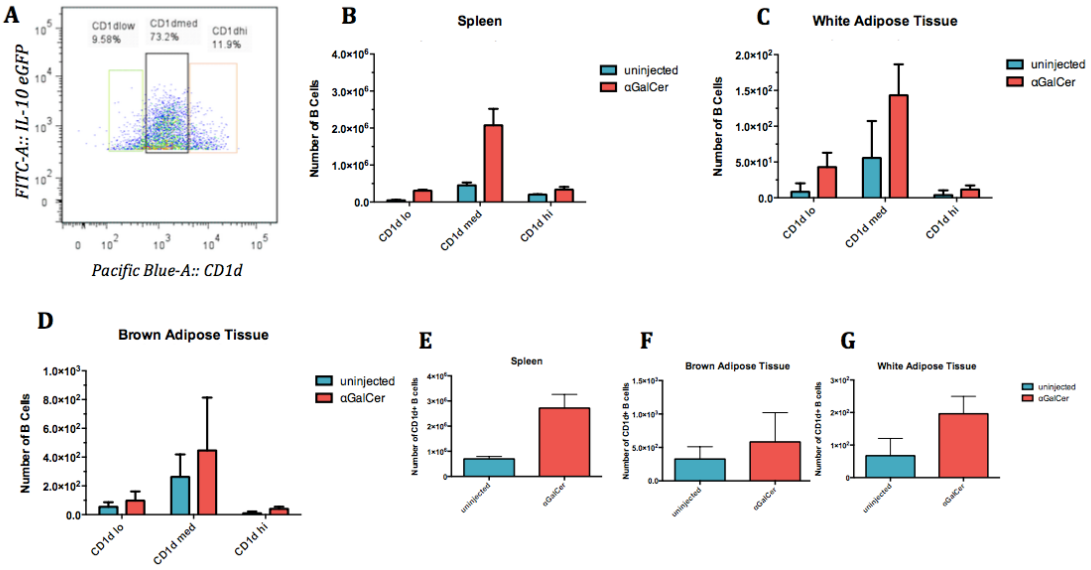

Figure 9 | IL-10 producing B cells and expression of CD1d increase in the spleen, white adipose tissue and brown adipose tissue following αGalCer injection. The cell counts were calculated from flow cytometry percentage data of CD1d^{+} B cells expressing IL-10 in VertX/Thy1.1 mice on day 4 following αGalCer injection. Red bars indicate mice that received αGalCer injection (n=3), blue indicates uninjected mice (n=3). The three groups of CD1d^{lo}, CD1d^{med}, and CD1d^{hi} were gated as shown in (**A**), for the spleen (**B**), white adipose tissue (**C**), and brown adipose tissue (**D**). The total mean number of IL-10^{+}CD1d^{+} B cells is shown in the spleen (**E**), brown adipose tissue (**F**) and white adipose tissue (**G**).

If regulatory B cells are positive for the CD1d receptor, this would suggest that iNKT cells and regulatory B cells could directly interact. IL-10 producing B cells expressing three different levels of CD1d expression were observed four days after αGalCer injection, so IL-10 positive B cells were split into three gates: CD1d^{lo}, CD1d^{med}, CD1d^{hi} (Figure 9A). Following αGalCer injection, the B cells in the spleen (Figure 9B), white adipose tissue (Figure 9C) and brown adipose tissue (Figure 9D) producing the highest levels of IL-10 were also CD1d^{med}. And it was this group of IL-10^{+}CD1d^{med} B cells which most notably increased in number following injection. However, especially in the white adipose tissue, this population of CD1d^{+} regulatory B cells is relatively small. The mean total number

of splenic CD1d^{+} regulatory B cells increased by 3.8 fold following αGalCer injection. In adipose tissue, there was a trend towards CD1d expression on B cells following αGalCer expression. In white adipose tissue the mean total population increased almost three fold, however in brown adipose tissue the mean total population increased by an insignificant amount.

Expansion of Splenic resident B cells after αGalCer injection requires iNKT cells

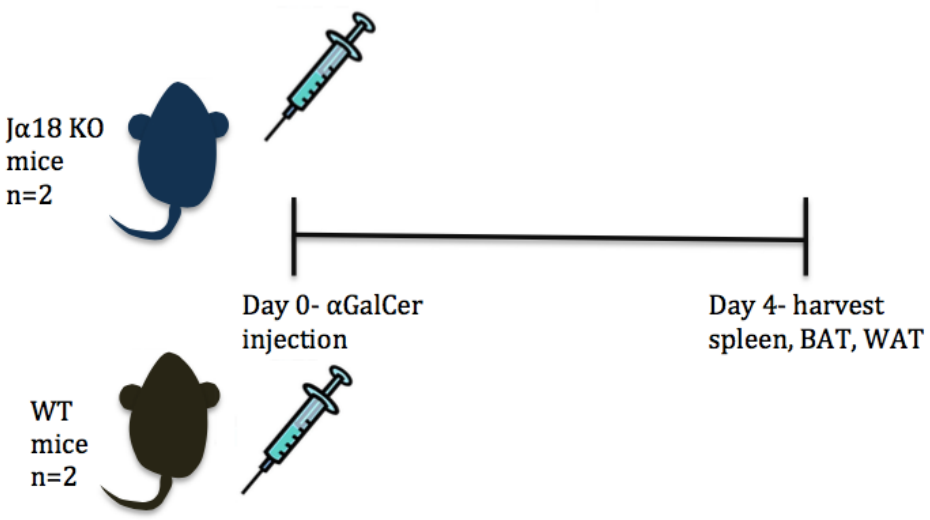

Figure 10 | Mice injection strategy with αGalCer in wild type C57BL/6 mice and Jα18 KO mice. Jα18 KO are deficient in invariant natural killer T cells. Two Jα18 KO mice and two wild type mice were injected on day 0 and tissue was harvest on day 4. Two uninjected Jα18 KO mice and two uninjected wild type mice were used as controls.

To further examine the interaction between iNKT cells and B cells, iNKT-deficient Jα18 knockout (KO) mice were utilized, and tissues were examined four days after αGalCer injection (Figure 10). iNKT and B cells were identified as previously described (Figure 4). As observed previously (Figure 6A), αGalCer injection stimulated an increase in the number of splenic-resident B cells in wild type mice (Figure 11A).

Loss of iNKT cells does not impact adipose B cell populations

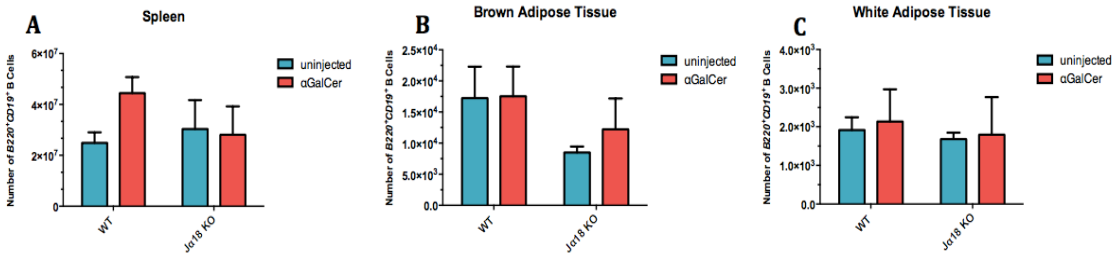

Figure 11 | B cell numbers following αGalCer injection are affected in the spleen (**A**) of Jα18 KO mice but not in the brown adipose tissue (**B**) or white adipose tissue (**C**). Red bars indicate mice that received αGalCer injection (n=2), blue indicates uninjected mice (n=2). The cell counts were calculated from flow cytometry percentage data on the B cell population in wild type and Jα18 KO mice.

However, αGalCer injection did not stimulate an increase in the number of resident splenic B cells in the iNKT-deficient Jα18 KO mice (Figure 11A), suggesting the splenic expansion is iNKT-dependent. In both brown and white adipose tissue, αGalCer injection did not stimulate an increase in tissue resident B cell numbers in wild type mice, or in iNKT-deficient Jα18 KO mice. Thus iNKT cells appear to have a direct role in the expansion of splenic B cells but not in the expansion of brown and white adipose B cells.

iNKT cells drive expansion of a B220^{+}CD19^{-} population following αGalCer stimulation

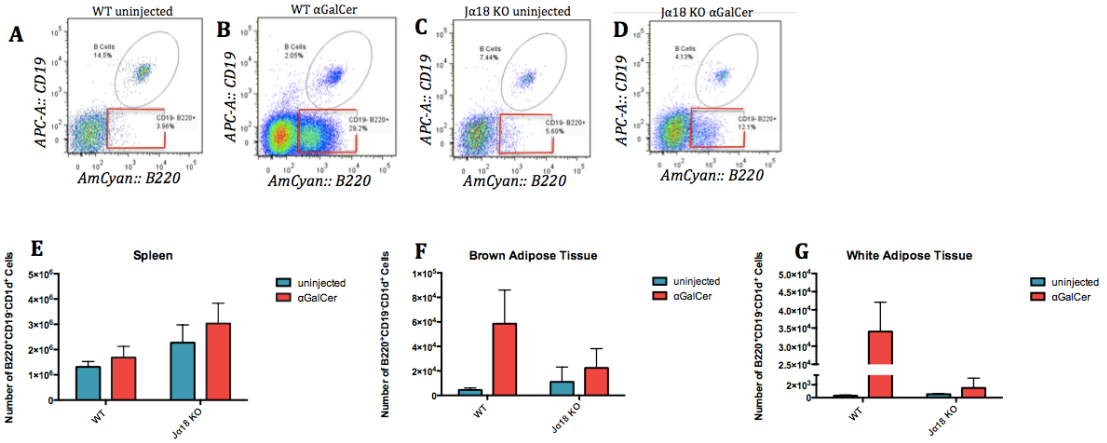

Figure 12 | Loss of iNKT cells negatively affects the B220^{+}CD19^{-} population in brown adipose tissue and white adipose tissue, but not in the spleen. The cell counts were calculated from flow cytometry percentage data on the CD19^{-}B220^{+} cell population in wild type and Jα18 KO mice. Red bars indicate mice that received αGalCer injection (n=2), blue indicates uninjected mice (n=2). (**A**) Wild type tissue uninjected, (**B**) wild type tissue injected with αGalCer, (**C**) Jα18 KO tissue uninjected, and (**d**) Jα18 KO tissue injected with αGalCer. The red gates show the affected B220^{+}CD19^{-} population. Graphs (**E-F**) show the B220^{+}CD19^{-} population of cells which are also expressing CD1d (**E**) The B220^{+}CD19^{-}CD1d^{+} population is less affected in the spleen, where αGalCer stimulation results in less of a population increase. (**F**) Brown adipose tissue and (**G**) white adipose tissue both display an increase in the B220^{+}CD19^{-} CD1d^{+} population following αGalCer stimulation, and both show deficiency in that population when iNKT cells are knocked out in the Jα18 KO mice.

In both the brown and white adipose tissues of wild type mice, injection of αGalCer results in an expansion of a B220^{+}CD19^{-} population of cells on day four post injection (Figure 12A, B). This expansion does not occur to the same extent in the spleens of wild type mice. In the adipose tissues of Jα18 KO mice, significantly less expansion of the B220^{+}CD19^{-} population occurs following αGalCer stimulation (Figure 12C, D). This suggests that expansion of the B220^{+}CD19^{-} cell population in response to αGalCer is iNKT-dependent. A significant portion of these B220^{+}CD19^{-} adipose cells also express CD1d, indicating that they have the potential to interact with iNKT cells. After gating the B220^{+}CD19^{-} population (Figure 12A-D), the population was then gated for CD1d^{+}

cells. The respective numbers of $B220^+CD19^-CD1d^+$ cells in the spleen, brown adipose tissue, and white adipose tissue are shown in Figure12 E-G. The population of $B220^+CD19^-CD1d^+$ cells in the spleen does not display any notable changes in response to αGalCer in both wild type and Jα18 KO mice (Figure 12E). In contrast, in the brown adipose tissue (Figure 12F) and in the white adipose tissue (Figure 12G), there is a significant increase in the $B220^+CD19^-CD1d^+$ cell population in wild type mice following αGalCer. However in the adipose tissue of the iNKT-deficient Jα18 KO mice there is little to no change in this same population of $B220^+CD19^-CD1d^+$ cells after αGalCer injection.

Discussion

Furthering an understanding of the interactions between iNKT cells and B cells in adipose tissue is critical to the study of obesity, autoimmune diseases and cancers. We examined iNKT cell and B cell interactions in brown and white adipose tissue, using the better-characterized interactions of these cells in the spleen as a means of comparison. Within adipose tissue, iNKT cell activation, as measured by an increase in tissue-resident iNKT and $IL\text{-}10^+$ iNKT cells, displays similar kinetics to iNKT cell activation in the spleen after αGalCer stimulation. However, we do not observe the same similarity in kinetics in B cell activation within adipose tissue and the spleen; while splenic B cells display iNKT-dependent proliferation and increase IL-10 production four days after αGalCer stimulation, we observed no significant change in population size or IL-10 production within adipose-resident B cells. Splenic B cells, have more potential to

directly interact with iNKT cells than adipose B cells, as they express higher levels of CD1d following αGalCer stimulation. Finally, we observed an iNKT-dependent expansion of $B220^{+}CD19^{-}CD1d^{+}$ cells specifically in adipose tissue and not in the spleen. Together, our data best support a model of innate (cognate) iNKT help in the spleen, and a model of adaptive (noncognate) iNKT help in adipose tissue, potentially via a $B220^{+}CD19^{-}CD1d^{+}$ cell (Figure 13).

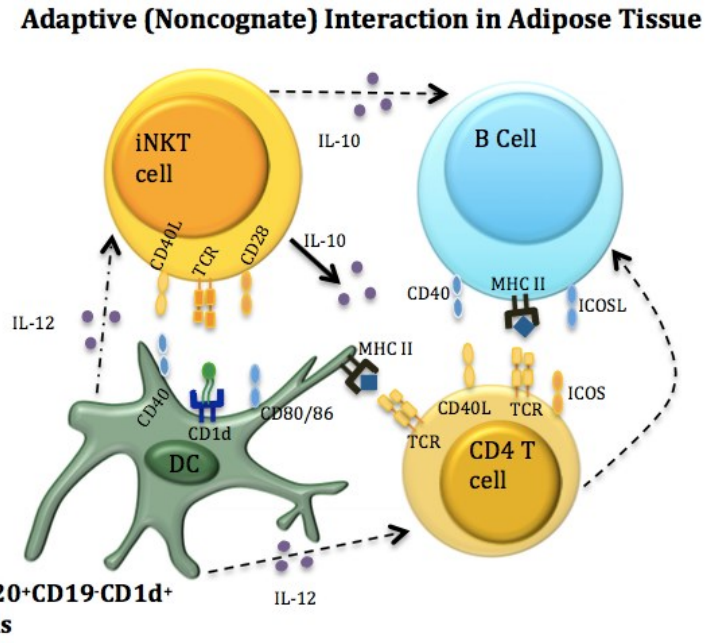

Figure 13 | Possible adaptive pathway for adipose iNKT cells. The $B220^{+}CD19^{-}CD1d^{+}$ cell population could potentially be dendritic cells, as shown in this diagram. iNKT cell production of IL-10 following αGalCer injection is clear, however the cells being acted upon by IL-10 is unknown.

Determining the identity and functionality of the $B220^{+}CD19^{-}CD1d^{+}$ cell population may be key in furthering our understanding of iNKT cell and B cell interactions in adipose tissue. This population of $B220^{+}CD19^{-}CD1d^{+}$ cells are most likely not macrophages which display high granularity, and thus should have been excluded from the lymphocyte gate. It is possible these are dendritic

cells, as they are antigen presenting cells which express CD1d and therefore are capable of interacting with iNKT cells. Dendritic cells have varying subsets, many of which have not been well described. Two dendritic cell populations previously described in mice, $CD11c^{high}B220^{neg}$ and $CD11c^{low}B220^{+}$, were both found to directly effect T cell populations (Bertola et al., 2012). Liver dendritic cells, which also were found to exhibit direct effects on the liver T cell population, have been described as $B220^{+}CD19^{-}$ (Lu et al., 2001). Bertola et al. (2012) described white adipose tissue dendritic cells as $CD11c^{high}B220^{neg}$ however, and reported finding no $B220^{+}$ dendritic cells. It is possible that αGalCer expands or recruits a novel, tissue-resident $B220^{+}$ subset of dendritic cells in brown and white adipose tissue, which is not found without αGalCer stimulation.

Our data suggests that within brown and white adipose tissue the primary pathway of interaction for adipose iNKT cells is the adaptive (or noncognate) pathway (Figure 13). Our findings show that the expansion of $B220^{+}CD19^{-}CD1d^{+}$ cells in adipose tissue is iNKT-dependent. This is consistent with an adaptive model for iNKT cell help to B cells. In the adaptive pathway for iNKT cell help to B cells, iNKT cells first activate dendritic cells, the dendritic cells activate $CD4^{+}$ T cells, and the $CD4^{+}$ T cells go on to activate B cells. In an adaptive pathway, the iNKT cells indirectly activate the B cells, and therefore it's likely that the kinetics for adaptive help differ from the kinetics for innate iNKT help. Thus future studies should focus on the kinetics of iNKT and B cell interactions in adipose tissue assuming an adaptive model, and examine later time points.

We also observed slight differences between the two varieties of adipose tissue tested. The brown adipose tissue had a larger increase in the $B220^{+}CD19^{-}$ $CD1d^{+}$ population following αGalCer injection, and more iNKT cells after αGalCer, but smaller numbers of $CD1d^{+}$ B cells than the white adipose tissue (Figure 8, Figure 9 & Figure 12). As the white adipose tissue had a larger population of $CD1d^{+}$ B cells, it is possible that iNKT cells in white adipose are providing some innate help for B cells. This difference in lymphocytes could perhaps be due to the different biological functions of the two adipose tissues as white adipose tissue serves as an energy store and brown adipose tissue is thermoregulatory. Given the small number of samples, it will be critical to examine these differences in more detail.

The limitations of these experiments were primarily that of size. The largest mice test group was three, and the smallest was two. In order to confirm the findings here with greater accuracy, experiments with more mice should be conducted. Additionally, without the specific markers for dendritic cells or macrophages it is impossible to identify the $B220^{+}CD19^{-}CD1d^{+}$ population of adipose cells. In order to examine the identity of these cells, markers for dendritic cells such as CD11c, and markers for macrophages such as F4/80 should be used. If the $B220^{+}CD19^{-}CD1d^{+}$ adipose cells truly are dendritic cells it would be interesting to examine mice deficient in iNKT cells and then reintroduce iNKT cells to see if this $B220^{+}CD19^{-}CD1d^{+}$ population can be rescued. Additionally, if the adipose tissue iNKT cells are providing adaptive help it would be beneficial to see if and when the adipose B cells are activated. If adaptive help from adipose

iNKT cells is occurring, we would expect to see class-switched antibody production by adipose B cells. Adipose B cells could be isolated and the constant region of their heavy chain could be sequenced in order to see if antibody class-switching had occurred. Another interesting future experiment would be to compare lean and obese mice in order to see what happens to the $B220^{+}CD19^{-}$ $CD1d^{+}$ cells in an obese model.

Gaining a clearer understanding of the mechanisms behind the activation of adipose tissue resident lymphocytes such as B cells, iNKT cells and dendritic cells has crucial implications for obesity and diabetes. It has been shown that in adipose tissue, activation of IL-10 producing iNKT cells increases the number of anti-inflammatory M2 adipose macrophages (Li et al., 2012). However within obese adipose tissue iNKT cell populations significantly decrease (Lynch et al., 2009). The loss of adipose iNKT cells results in an increase of pro-inflammatory M1 adipose macrophages (Lynch et al., 2014). These adipose M1 macrophages contribute to insulin insensitivity and resistance by reducing glucose uptake by adipocytes and modifying adipocyte functionality (Zhang et al., 2015). Thus a self-perpetuating pro-inflammatory cycle begins in obese adipose tissue. However, activation of iNKT cells in obese adipose tissue can result in production of anti-inflammatory signals, improved lipid storage, better insulin sensitivity and loss of weight (Lynch et al., 2012). Therefore study of the activation of adipose iNKT cells, dendritic cells and B cells could be applied to therapies and treatments for obesity, and preventative measures for diabetes. Our results suggest that iNKT cells in adipose tissue are providing adaptive help, which

involves additional layers of regulation, and thus delayed kinetics. However adaptive iNKT cell help does result in the creation of memory B cells and class-switched antibody producing plasma cells. This would indicate that within both brown and white adipose tissue the adaptive help provided by adipose iNKT cells serves to combat antigen specific inflammation.

Materials and Methods

Mice

C57BL/6 mice, C57BL/6 *Cxcr6* $^{GFP/-}$ mice, C57BL/6.VertX/Thy1.1 mice, C57BL/6.Jα18 KO mice and C57BL/6.4get/Kn2 Cre mice were all obtained from Jackson Laboratory. All mice strains were kept in pathogen free facilities at Trudeau Institute. αGalCer (0.5 μg) was administered intravenously in <0.01% DMSO/PBS. The C57BL/6.4get/Kn2 Cre mice were previously infected with Heligmosomoides polygyrus orally, and were used for eGFP compensation in the experiments using C57BL/6.VertX/Thy1.1 mice. 8-20 week old male mice were used in all experiments. All work with animals was approved by the Trudeau Institute's Institutional Animal Care and Use Committee.

Reagents

The following reagents were used in these studies: Propidium Iodide (PI), anti-CD1d BV421, anti-CD19 APC, anti-IgM Pe-Cy7, anti-CD25 PE, anti-B220 APC-Cy7, anti-FR4 PE, anti-PD1 Pe-Cy7, CD1d Tetramer PE (NIH Tetramer Core Facility), anti-TCRβ APC-Cy7, anti-NRP1 BV421, anti-CD11b FITC, Hoechst, FC receptor blocking antibody, anti-CD4 APC, anti-IgD FITC, and red

blood cell lysis buffer. With the exception of the CD1d Tetramer all reagents were obtained from eBiosciences, BioLegend or BD Biosciences.

Confocal Images

Epididymal adipose (white adipose tissue), intra-scapular brown adipose and splenic tissue samples were harvested from the mice. The white adipose tissue was cut into three sections and placed in wells with 0.02% sodium azide and 5% normal mouse serum in phosphate buffered saline (PBS). Brown adipose tissue samples and spleens were embedded in an agarose gel and cut into thin slices with a Leica VT1200 Vibratome. These sections were then placed in PBS and mouse serum. CD1d Tetramer stain was added first to samples, then the rest of antibody cocktail was added. Tissue samples were then placed on glass slides with Aqua Poly/Mount and a coverslip. Samples were visualized using a Leica TCS SP5 confocal microscope.

Isolation of Immune Cells

Spleens were strained through metal strainer, washed with 2% bovine serum albumin (BSA) in PBS and red blood cells were lysed. Single-cell suspensions were then washed with PBS, centrifuged and resuspended in 5 ml 2% BSA in PBS. Cells were then counted using Trypan Blue staining.

Epididymal (white) adipose tissue and intra-scapular brown adipose tissue were harvested following PBS perfusion of the circulatory system via hepatic portal vein cut. Adipose tissue was then minced dry.

Collagenase IV and VIII were compared for efficiency and yield in the isolation of stromal vascular cells using flow cytometry data of B cell and iNKT

cell percentages, and Trypan blue cell count estimations. Collagenase IV solution with 5% fetal calf serum (FCS) yielded higher total cell counts and higher numbers of B cells and iNKT cells, and was thus used throughout for the rest of the trials.

Collagenase IV solution was used to rinse minced tissue into 50 ml conical tubes. Collagenase IV solution contained 0.2 mg/ml Collagenase IV in 20 ml RPM1+ 5% FCS per sample. Tubes containing minced solutions were then placed in a rotational shaker for 1 hour at 37C. Samples were then passed through 100 μm filter into new 50 ml conical tube. Samples were then centrifuged for 5 min at 4C. The supernatant containing adipocytes was aspirated off. The cell pellet from the brown adipose tissue was treated with red blood cell lysis buffer to remove red blood cell contamination. The cell pellet from the white adipose tissue was not treated with red blood cell lysis buffer to avoid losing cells. Samples were resuspended in single-cell suspensions.

Flow Cytometry

Samples were treated with Fc receptor-blocking antibody, then stained with CD1d-Tetramer. Remaining antibody cocktail stains were added next. Samples were washed with PBS + 2% BSA. Propidium Iodide was then added to all samples to exclude dead cells. A three-laser BD FACSCanto II was used to analyze the samples and FlowJo software was used to interpret the data.

Data Analysis and Statistics

GraphPad Prism (version 6) and Microsoft Excel (version 14.4.1) were used to analyze and format the data sets, and calculate mean and standard deviation. Note that standard error was not calculated due to low sample size.

Acknowledgements

I am so grateful to the Trudeau Institute and my primary investigator Liz Leadbetter for giving me the opportunity of a lifetime. I would like to thank Katja Mohrs, Paula Lanthier and Jen Yates for teaching me so much and being incredible friends. I'm so thankful for my thesis advisor Olivia Hatton, for constantly pushing me to strive for better. I would also like to thank Darrell Killian for being a great secondary thesis advisor. And many thanks to Donna and Kelley for the endless snacks. I would like to thank my family and friends (especially Abby, Ana, Anna, Emma & Brittany) for all their love and support.

References

Apostolopoulos, V., de Courten, M.P., Stojanovska, L., Blatch, G.L., & de Courten, B. (2015). The complex immunological and inflammatory network of adipose tissue in obesity. *Molecular Nutrition & Food Research*, [Epub ahead of print]

Bertola, A., Ciucci, T., Rousseau, D., Bourlier, V., Duffaut, C., Bonnafous, S., … Wakkach, A. (2012). Identification of Adipose Tissue Dendritic Cells Correlated With Obesity-Associated Insulin-Resistance and Inducing Th17 Responses in Mice and Patients. *Diabetes*, *61*(9), 2238–2247.

Betz, M., Enerback, S. (2015). Human brown adipose tissue: what we have learned so far. *Diabetes, 64*(7), 2352-2360.

Chang, P., Barral, P., Fitch, J., Pratama, A., Ma, C.S., Kallies, A., Hogan, J.J., Cerundolo, V., Tangye, S., Bittman, R., Brink, R., Godfrey, D., Batista, F.D., Vineusa, C.G. (2011). Identification of Bcl-6 dependent follicular helper NKT cells that provide cognate help for B cell responses. *Nature Immunology, 13*(1), 35-43.

Chaudhry, M. S., & Karadimitris, A. (2014). Role and regulation of CD1d in normal and pathological B cells. *Journal of Immunology (Baltimore, Md. : 1950)*, *193*(10), 4761–4768.

Exley, M., Hand, L., O'Shea, D., Lynch, L. (2014). Interplay between the immune system and adipose tissue in obesity. *Journal of Endocrinology, 223*(2), R41-R48.

Huang, S., Fu, R., Shyu, W., Liu, S., Jong, G., Chiu, Y., Wu, H., Tsou, Y., Cheng, C., Lin, S., (2013). Adipose-derived stem cells: isolation, characterization, and differentiation potential. *Cell Transplantation, 22*(4), 701-709.

Ji, Y., Sun, S., Xu, A., Bhargava, P., Yang, L., Lam, K. S. L., … Qi, L. (2012). Activation of Natural Killer T Cells Promotes M2 Macrophage Polarization in Adipose Tissue and Improves Systemic Glucose Tolerance via Interleukin-4 (IL-4)/STAT6 Protein Signaling Axis in Obesity. *The Journal of Biological Chemistry*, *287*(17), 13561–13571.

Leadbetter, E., King, I., Fortier, A., Tighe, M., Dibble, J., Watts, G., Veerapen, N., Haberman, A., Besra, G., Mohrs, M., Brenner, M. (2011). Invariant natural killer T cells direct B cell responses to cognate lipid antigen in an IL-21-dependent manner. *Nature Immunology. 13*(1), 10.1038/ni.2172.

Leadbetter, E., Vomhof-DeKrey, E., Yates, J. (2014). Invariant NKT cells provide innate and adaptive help for B cells. *Current Opinion in Immunology, 28,* 12-17.

Lu, L., Bonham, C.A., Liang, X., Chen, Z., Li, W., Wang, L., Watkins, S.C., Nalesnik, M.A., Schlissel, M.S., Demestris, A.J., Fung, J.J., QIan, S. (2001). Liver-derived DEC205+B220+CD19- dendritic cells regulate T cell responses. *Journal of Immunology, 166*(12), 7042-7052.

Lynch, L., Michelet, X., Zhang, S., Brennan, P., Moseman, A., Lester, C., Besra, G., Vomhof-DeKrey, E., Tighe, M., Koay, H., Godfrey, D., Leadbetter, E., Sant'Angelo, D., von Andrian, U., Brenner, B. (2014). Regulatory iNKT cells lack expression of the transcription factor PLZF and control the homeostasis of Treg cells and macrophages in adipose tissue. *Nature Immunology, 6*(1), 85–95

Lynch, L., Nowak, M., Varghese, B., Clark, J., Hogan, A., Toxavidis, V., Balk, S., O'Shea, D., O'Farrelly, C., Exley, M. (2012). Adipose tissue invariant NKT cells protect against diet-induced obesity and metabolic disorder through regulatory cytokine production. *Immunity, 37,* 574-587.

Lynch, L., O'Shea, D., Winter, D.C., Geoghengan, J., Doherty, D.G., O'Farrelly, C. (2009). Invariant NKT cells and CD1d(+) cells amass in human omentum and are depleted in patients with cancer and obesity. *European Journal of Immunology, 39*(7), 1893-1901.

Macho-Fernandez, E., Cruz, L., Ghinnagow, R., Fontaine, J., Bialecki, E., Frisch, B., Trottein, F., & Faveeuw, C. (2014). Targeted delivery of α-Galactosylceramide to CD8α$^+$ Dendritic Cells Optimizes Type I NKT Cell–Based Antitumor Responses. *The Journal of Immunology, 193*(2), 961-969.

Nikolic, T., Dingjan, G.M., Leenen, P.J., & Hendriks, R.W. (2002). A subfraction of B220(+) cells in murine bone marrow and spleen does not belong to the B cell lineage but has dendritic cell characteristics. *European Journal of Immunology, 32*(3), 686-692.

Nishimura, S., Manabe, I., Tataki, S., Nagasaki, M., Otsu, M., Yamashita, H., Sugita, J., Yoshimura, K., Eto, K., Komuro, I., Kadowaki, T., Nagai, R. (2013). Adipose natural regulatory B cells negatively control adipose tissue inflammation. *Cell Metabolism, 18,* 759-766.

Madan, R., Demircik, F., Surianarayanan, S., Allen, J., Divanovic, S., Trompette, A., Yogev, N., ... Karp, C. (2009). Nonredundant roles for B cell-derived IL-10 in immune counter regulation. *Journal of Immmunology, 183,* 2312-2320.

Magalhaes, I., Kiaf, B., & Lehuen, A. (2015). iNKT and MAIT Cell Alterations in Diabetes. *Frontiers in Immunology*, *6*, 341.

Matsushita, T., Tedder, T.F. (2010). Identifying regulatory B cells (B10 cells) that produce IL-10 in mice. *Methods in Molecular Biology, 677*, 99-111.

Nicol, A., Tazbirkova, A., Nieda, M, (2011). Comparison of clinical and immunological effects of intravenous and intradermal administration of α-GalactosylCeramide (KRN7000)-pulsed dendritic cells. *Clinical Cancer Research, 17*(15)*,* 5140-5151.

Nutt, S., Hodgkin, P., Tarlinton, D., Corcoran, L. (2015). The generation of antibody-secreting plasma cells. *Nature Reviews Immunology, 15,* 160-171.

Park, A., Kon Kim, W., Bae, K. (2014). Distinction of white, beige and brown adipocytes from mesenchymal stem cells. *World Journal of Stem Cells, 6*(1), 33-42.

Recaldin, T. & Fear, D.J. (2015). Transcription factors regulating B cell fate in the germinal centre. *Clinical & Experimental Immunology,* [Epub ahead of print]

Singh, A. K., Wilson, M. T., Hong, S., Olivares-Villagómez, D., Du, C., Stanic, A. K., … Van Kaer, L. (2001). Natural Killer T Cell Activation Protects Mice Against Experimental Autoimmune Encephalomyelitis. *The Journal of Experimental Medicine*, *194*(12), 1801–1811.

Tard, C., Rouxel, O., Lehuen, A. (2015). Regulatory role of natural killer T cells in diabetes. *Biomedical Journal,* [Epub ahead of print]

Tedder, T. (2015). B10 cells: a functionally defined regulatory B cell subset. *Journal of Immunology, 194,* 1395-1401.

Valina, C., Pinkernell, K., Song, Y., Bai, X., Sadat, S., Campeau, R., Jemtel, T., Alt, E. (2007). Intracoronary administration of autologous adipose-tissue-dervied stem cells improves left ventricular function, perfusion, and remodeling after acute myocardial infartion. *European Heart Journal, 28*, 2667-2677.

Wentworth, J. M., Naselli, G., Brown, W. A., Doyle, L., Phipson, B., Smyth, G. K., … Harrison, L. C. (2010). Pro-Inflammatory $CD11c^{+}CD206^{+}$ Adipose Tissue Macrophages Are Associated With Insulin Resistance in Human Obesity. *Diabetes*, *59*(7), 1648–1656.

Wu, C., Cheng, W., Sun, Y., Dang, Y., Gong, F., Zhu, H., … Zhu, Z. (2014). Activating Brown Adipose Tissue for Weight Loss and Lowering of Blood Glucose Levels: A MicroPET Study Using Obese and Diabetic Model Mice. *PLoS ONE*, *9*(12), e113742. http://doi.org/10.1371/journal.pone.0113742
Zhang, Y., Shi, L., Mei, H., Zhang, J., Zhu, Y., Han, X., & Zhu, D. (2015). Inflamed macrophage microvesicles induce insulin resistance in human adipocytes. *Nutrition & Metabolism*, *12*, 21.